INTERFERENCE ALIGNMENT USING NI FLEXRIO

N. Prasanth Anthapadmanabhan, J. Saul Duran, Kyle Miller, Vidur Bhargava
(University of Texas at Austin, Austin, TX, USA;
{anprasanth, jsduran, kyletmiller, vidurbhargava}@mail.utexas.edu);
Takao Inoue, Ahsan Aziz (National Instruments, Austin, TX, USA;
{takao.inoue, ahsan.aziz}@ni.com); and Sriram Vishwanath
(University of Texas at Austin, Austin, TX, USA; sriram@ece.utexas.edu)

ABSTRACT

Interference Alignment (IA) is a fresh and exciting interference management technique for wireless networks. IA promises a linear increase in throughput with the number of users in a wireless system, and is known to be capacity optimal for classes of wireless networks. The current promise of IA is in theory, with limited practical literature in existence to verify these claims. This paper represents one of the first efforts to understand the true potential of interference alignment in practical wireless systems.

1. INTRODUCTION

The number and types of wireless-featured devices is steadily growing thus placing a heavy demand on limited available spectrum. Interference between these devices can significantly degrade performance and reduce the throughput per user. Therefore, the key to improving the performance of wireless systems lies in managing interference effectively.

Interference alignment (IA) is a new and exciting physical layer technique [1], [2] that promises significant improvements in throughput. This alignment in signals can be induced after coding and modulation in the transmit chain of a traditional communication system. Fundamentally, the concept of alignment is to extend modulated symbols to a higher dimensional space such that the interfering signals are all aligned and occupy the smallest subspace at each receiver. In this case, the remaining dimensions can be used to receive the desired signal essentially free of interference. Note that IA is not the same as spread spectrum, multiple access schemes or other interference minimization or avoidance schemes. IA makes no attempt to avoid, cancel or minimize interference. Instead, it aims to align the interference along dimensions that are different from that of the signal. As such, it has been found to perform much better than all the existing interference management schemes.

In theory, IA can achieve a sum throughput that increases linearly with the number users [1]. Note that this is quite amazing, as traditional time or frequency division multiple access schemes have no increase in throughput, and each user only obtains a fraction of the total throughput which decreases with increasing number of users in the system.

It is important to emphasize that this result is a theoretical one, and significant work yet needs to be done to bring the growing body of literature to practice. The theoretical benefits of IA are based on a set of assumptions (such as perfect channel state knowledge and/or other ideal requirements) which may or may not be feasible in practice. There is a limited literature [3], [4] on testing the viability of IA on hardware, and this literature indicates that it is indeed of practical value. The paper [3] considers a narrow-band experiment setup where synchronization issues do not arise and in addition channel information needs to be exchanged among users. In [4], channel measurements are collected and used offline to estimate the performance of IA.

Our ultimate goal is to go beyond the limited existing body of literature to a full blown implementation to show that IA is indeed feasible. We do this using a software-defined radio (SDR) platform from National Instruments (NI). In this paper, we present our results from a hardware implementation of a technique known as *blind interference alignment* which was recently proposed in the literature [5].

2. BLIND INTERFERENCE ALIGNMENT

IA algorithms, in general, require *perfect global channel knowledge* (i.e., perfect knowledge of all the channel coefficients in the system) at all the transmitters and receivers. But, this requirement is impractical for most real systems. In [5], the authors proposed a novel technique known as *blind interference alignment* which eliminates the need for any channel knowledge at the transmitters. However, this comes at the price of the practical challenge of implementing the re-

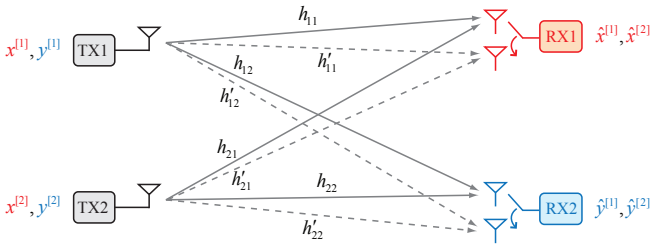

Figure 1: System model

ceivers with a *reconfigurable antenna*. In this section, we provide a short description of the theory behind the blind IA technique, while challenges in practical implementation are detailed later in Section 4.

In our experiment setup, we consider two transmitters (TX1 and TX2) and and two receivers (RX1 and RX2) as shown in Fig. 1. Each transmitter $i = 1, 2$ has two messages $x^{[i]}, y^{[i]} \in \mathbb{C}$ which need to be recovered at RX1 and RX2 respectively. This is commonly referred to as the X-channel. Although the blind IA scheme is more general, we focus our attention below to the specific 2-transmitter 2-receiver setup.

In the blind IA scheme, each receiver is equipped with a reconfigurable antenna which can switch between two different receive modes, but the receivers have only one RF chain. The receivers switch modes based on a pre-determined pattern known to everyone. For $i, j \in \{1, 2\}$, let $h_{ij} \in \mathbb{C}$ and $h'_{ij} \in \mathbb{C}$ denote the coefficient of the channel between transmitter i and receiver j with the receive mode set to 1 and 2 respectively. The channel coefficients have a generic (non-degenerate) continuous probability distribution. It is assumed that the channel stays constant across a "supersymbol", which constitutes three transmission slots.

At time instant t, suppose that $u^{[1]}(t), u^{[2]}(t) \in \mathbb{C}$ are transmitted from TX1 and TX2 respectively. In this case, the received signal at user j using receive mode 1 is given by

$$z^{[j]}(t) = h_{1j}u^{[1]}(t) + h_{2j}u^{[2]}(t) + w^{[j]}(t), \qquad (1)$$

where $w^{[j]}(t) \sim \mathcal{CN}(0, \sigma^2)$ is the additive white Gaussian noise (AWGN). The received signal using mode 2 is obtained analogously using the channel coefficients h'_{1j} and h'_{2j} in (1). The transmitters have absolutely no knowledge of the channel state. On the other hand, each receiver j is assumed to know only the local channel coefficients h_{1j}, h_{2j}, h'_{1j} and h'_{2j}.

Recall that transmitter i has two messages $x^{[i]}, y^{[i]} \in \mathbb{C}$ intended for RX1 and RX2 respectively. Assuming perfect synchronization between the transmitters and receivers, the blind IA scheme operates in 3 time slots as shown in Table 1.

In time slot 1, each transmitter sends the sum of its two messages, while in time slots 2 and 3 the messages for RX1

Table 1: Transmitted symbols and receiver switching in blind IA

Time Slot	1	2	3
Transmit	$x^{[i]} + y^{[i]}$	$x^{[i]}$	$y^{[i]}$

Time Slot	1	2	3
RX1	mode 1	mode 2	mode 1
RX2	mode 1	mode 1	mode 2

and RX2 are transmitted separately. The receivers switch between the two receive modes according to the pattern shown in Table 1. Due to the symmetry, the recovery process is analogous at the two receivers, and so we focus on RX1 below. The received signal $z^{[1]}(t)$ at RX1 over the three time slots, assuming the channel remains constant, is given by

$$\begin{aligned} z^{[1]}(1) &= h_{11}(x^{[1]} + y^{[1]}) + h_{21}(x^{[2]} + y^{[2]}) + w^{[1]}(1), \\ z^{[1]}(2) &= h'_{11}x^{[1]} + h'_{21}x^{[2]} + w^{[1]}(2), \\ z^{[1]}(3) &= h_{11}y^{[1]} + h_{21}y^{[2]} + w^{[1]}(3). \end{aligned}$$

Note that we have used the fact that RX1 switches to mode 2 for the second time slot. We now take advantage of the particular manner in which the interfering and desired signals are aligned in order to remove (i.e., zero-force) the interference and obtain the following system of equations:

$$\begin{pmatrix} z^{[1]}(1) - z^{[1]}(3) \\ z^{[1]}(2) \end{pmatrix} = \begin{pmatrix} h_{11} & h_{21} \\ h'_{11} & h'_{21} \end{pmatrix} \begin{pmatrix} x^{[1]} \\ x^{[2]} \end{pmatrix} + \begin{pmatrix} w^{[1]}(1) - w^{[1]}(3) \\ w^{[1]}(2) \end{pmatrix}. \qquad (2)$$

Since the channel coefficients are chosen from a continuous distribution, the channel vectors involved in (2) are linearly independent with high probability. Therefore, RX1 can recover the desired messages $x^{[1]}$ and $x^{[2]}$.

A high- signal to noise ratio (SNR) performance metric of wireless networks is its degrees of freedom (DoF). DoF is defined as $\lim_{\text{SNR}\to\infty} C_{\text{sum}}(\text{SNR})/\log \text{SNR}$, where $C_{\text{sum}}(\text{SNR})$ denotes the maximum sum throughput achievable in the network. Thus, DoF denotes the asymptotic growth rate of throughput with SNR. Using the alignment scheme described above, we find that we can achieve a DoF of $\frac{4}{3}$. It has been shown that this is, in fact, the optimal DoF for this channel [6]. Thus, alignment promises in theory to achieve rates that are significantly larger than other schemes in existence.

We make a brief remark on how the blind IA scheme scales as the system size increases. In general, if there are

M transmitters and K receivers, then each receiver requires a reconfigurable antenna that can switch between M modes. Furthermore, a supersymbol of length $(M-1)^K + K(M-1)^{K-1}$ symbols would be required in this situation.

3. EXPERIMENT SETUP

The theoretical promise of IA schemes is based on certain assumptions including perfect global channel knowledge at all transmitters and receivers, perfect synchronization of all users, and favorable channel coherence structure. Although the blind IA technique (cf. Section 2) dispenses with the requirement of channel knowledge at transmitters, other assumptions still remain, and in addition, this comes at the cost of additional receiver complexity in the form of receive mode switching. In this paper, we develop a non-realtime implementation of the blind IA scheme in an indoor environment. Our setup serves to verify the practical feasibility of blind IA and also provides measures of its actual performance. In this way, we take the first step in this paper towards a completely realtime implementation.

3.1. Implementation Challenges

A crucial challenge in implementing the blind IA scheme is ensuring synchronization (in time and frequency) between the two transmitters and the two receivers. This challenge is further exacerbated by the requirement for receive mode switching which occurs in synchronized time slots. Furthermore, switching from one receive mode to another will involve a time delay in reality which must be accounted for.

Recall also that blind IA requires the channel to stay constant over three time slots. In a practical implementation, this imposes the restriction that the time slots are of short duration. On the other hand, reducing the time slot duration necessitates faster speeds for receiver switching as a consequence.

3.2. Setup and Parameters

We use NI's SDR platform which consists of a PXIe-8130 real-time controller, PXIe-7965R FlexRIO FPGA module with Xilinx Virtex 5 sx95T, NI-5781 100M samples/sec baseband transceiver, and Ettus Research XCVR2450 daughterboard. One set of these modules constitutes one unit of a transmitter or a receiver. The PXIe cards are mounted on the PXIe-1082 8-slot chassis with high speed PXI-Express backplane bus. The hardware configuration is shown in Fig. 2. The PXIe-8130 is an AMD Turion 64 based controller running real-time operating system. A graphical design environment, LabVIEW, is used to design and program the controller,

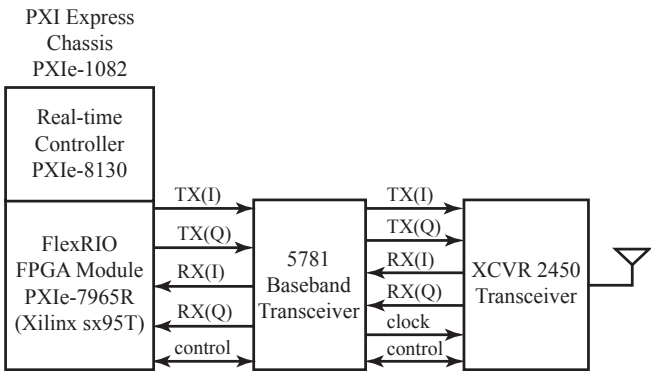

Figure 2: NI's SDR platform using FlexRIO

Table 2: System parameters

BW (MHz)	1.4	3	5	10	15	20
N subcarriers	72	180	300	600	900	1200
Subcarrier spacing	15 kHz					
# nulled subcarriers	12					
CP length	16.67 μs					
Symbol duration	$\frac{1}{12}$ ms					

making it a true software defined platform.

We use OFDM modulation with QPSK signaling over the 2.4 GHz ISM band with center frequency set at 2.437 GHz. The parameters for OFDM modulation are given in Table 2 and are chosen based on the LTE standard [7]. The 12 subcarriers centered at DC are nulled resulting in $N' = N - 12$ data subcarriers.

Our setup employs three PXIe-1082 chassis each running a real-time operating system. Two FlexRIO SDRs are installed on the first chassis and function as the transmitters TX1 and TX2. The remaining two chassis each have a FlexRIO SDR installed and play the role of RX1 and RX2 respectively. A local area network is used to network the three chassis to a development computer running LabVIEW. The OFDM signal generation and IA computation are performed on the real-time controller. The FlexRIO FPGA module is used to perform the fine grain symbol timing adjustment and sample rate conversion to transmit or receive the signal from the baseband transceiver.

3.3. Receive Mode Switching and Synchronization

We provide for two different receive modes by connecting the Ettus XCVR2450 daughterboards at the receivers to two

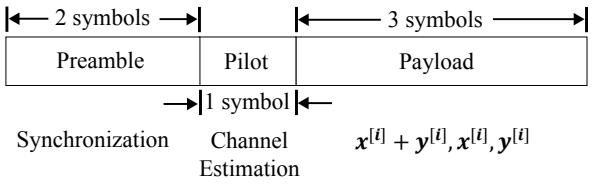

Figure 3: Frame structure

separate antennas with sufficient distance separation (at least 7 cm) to guarantee independent channel realizations. Nevertheless, both antennas share the same RF chain. The receiver switches between the two antennas using the antenna selection feature onboard the XCVR2450.

The transmitters TX1 and TX2, which are mounted on the same chassis, are first synchronized (in time and frequency) by taking advantage of the triggering functionality and the 10 MHz backplane reference clock of PXIe-1082 [8]. Synchronizing the receivers and the switching of antennas, on the other hand, is a much more intricate problem. Therefore, we carefully design our experiment to alleviate these challenges, while still exactly emulating the blind IA scheme. Our design is explained in the next two subsections.

3.4. Transmitter

The operation of transmitter i is illustrated in Fig. 4. Each transmitter generates two streams of $2N'$ pseudo-random bits, which are then padded to generate $2N$ bits. These bits are modulated using QPSK signaling to obtain N samples $\boldsymbol{x}^{[i]} = (x_1^{[i]}, \ldots, x_N^{[i]})$ and $\boldsymbol{y}^{[i]} = (y_1^{[i]}, \ldots, y_N^{[i]})$ destined for RX1 and RX2 respectively. The IA precoding step arranges the samples according to Table 1. This step results in a payload of $3N$ samples $\boldsymbol{x}^{[i]} + \boldsymbol{y}^{[i]}, \boldsymbol{x}^{[i]}, \boldsymbol{y}^{[i]}$. To this payload, $2N$ samples of preamble and N samples of pilots are are added. We note that our pilot pattern, used for channel estimation, is orthogonal in frequency for TX1 and TX2 by loading the odd and even subcarriers respectively. Finally, the samples are OFDM modulated to construct a frame of length 6 OFDM symbols (0.5 ms) as shown in Fig. 3. Once the output frame is constructed, TX1 and TX2 transmit their corresponding frames repeatedly and in a synchronous manner until both receivers are able to decode. This process emulates blind IA, while facilitating switching and synchronization at the receivers as explained below.

3.5. Receiver

The receiver operation is illustrated in Fig. 5. First, the receiver captures the entire transmitted frame using antenna 1. Next, antenna 2 is selected and the process is repeated. Observe that we exploit the transmitter's repetition of frames in choosing the above switching method. In fact, the actual blind IA requires that antenna switching to be done at symbol interval which is challenging. Our design allows us to evaluate the performance of blind IA without stringent switching times and synchronization. The preamble is used to detect the start of the frame and perform frequency offset correction using the Schmidl-Cox algorithm [9]. The rest of the frame is then demodulated to obtain the received reference signal and the $3N'$ payload samples. Channel estimation is performed in frequency domain via linear interpolation. The IA decoding uses equation (2) to recover the $2N'$ payload data. Finally, the channel estimate obtained using the pilots are used in ML detection to recover the transmitted bits.

4. RESULTS

In this section, we present the results from our implementation of blind IA on NI's SDR platform. Furthermore, we also compare the performance of blind IA against that of a traditional time-division scheme. We first describe the time-division setup before proceeding to the results.

4.1. Time-division scheme

We consider the same physical setup as shown in Fig. 1 for blind IA. However, in the time-division scheme, the transmitters TX1 and TX2 now take turns in sending messages to the desired receivers and thus there is no interference. Since the receivers are equipped with two antennas in our physical setup, a total of 8 point-to-point links are possible between the transmitters and the receivers. In our time-division setup, we assume that each of these 8 links is allocated an equal amount of time. Thus the performance of the time-division scheme would simply be the average of the performance of the 8 point-to-point links.

In order to make a direct comparison with the blind IA scheme, we use the same modulation scheme and frame structure (Fig. 3) as in blind IA. The only difference is in the payload field of the frame. In the time-division scheme, we transmit 3 OFDM symbols $\boldsymbol{x}_1^{[ij]}, \boldsymbol{x}_2^{[ij]}, \boldsymbol{x}_3^{[ij]}$, on the link from transmitter i to receiver j, where each symbol carries $2N'$ independent data bits.

4.2. Results and Discussion

In this section, our experimental results for bit error rate (BER) as a function of the SNR are shown for $N = 600$ subcarriers. The BER is computed over 1000 received packets in each case. In Fig. 6a, we plot the individual BER curves

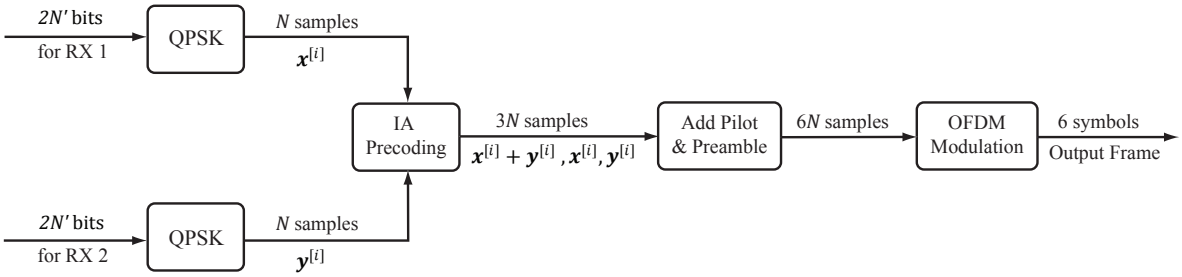

Figure 4: Block diagram of the transmitter

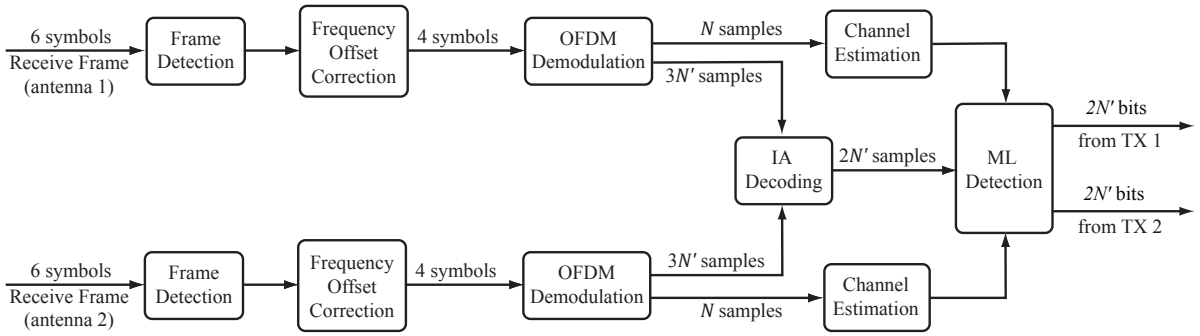

Figure 5: Block diagram of the receiver

for receivers RX1 and RX2 while using the blind IA scheme. Fig. 6b shows the results for the time-division scheme by taking two point-to-point links - TX1 to RX1 antenna 1 and TX2 to RX1 antenna 1 - as an example. In Fig. 6c, we compare the average BER (with respect to RX1 and RX2) for blind IA with the BER for the time-division scheme (obtained by averaging the BER performance of the 8 point-to-point links). Interestingly, we find that blind IA has a lower BER for smaller values of SNR. This can be explained by the observation that the preamble has twice the power in blind IA due to its simultaneous transmission from both TX1 and TX2. This enables improved synchronization at the receiver. However, the BER flattens out around 10^{-3} for higher SNR in the case of IA, while very low values are obtained for time-division. We believe this is because the interference from the other transmitter becomes dominant in this situation.

In addition, we also plot the normalized (effective) sum rate R_{sum} (in bits/s/Hz) which is measured as follows. First, observe that in blind IA we transmit a total of $4 \times 2N'$ bits in 3 symbol durations using a bandwidth of $N \cdot \Delta f$, where $\Delta f = 15$ kHz denotes the subcarrier spacing. A fraction $(1-\text{BER}_{IA})$ of the transmitted bits are received without error on average resulting in a normalized sum rate of

$$R_{\text{sum}}^{IA} = \frac{4}{3} \times \frac{2N'}{TN\Delta f}(1 - \text{BER}_{IA}),$$

where $T = 1/12$ ms and $\Delta f = 15$ kHz. Similarly, the normalized (effective) sum rate for time-division is obtained as

$$R_{\text{sum}}^{TD} = \frac{2N'}{TN\Delta f}(1 - \text{BER}_{TD}).$$

We observe that there is a clear gain in the normalized sum rate by using IA as opposed to time-division.

5. CONCLUSIONS AND FUTURE RESEARCH

The increased throughput from interference alignment can provide a possible solution to the conundrum of satisfying the increasing data rate demands with the limited spectrum available. Thus, the practical feasibility of interference alignment could significantly alter the way wireless devices are designed in the future. Indeed, IA can cause a major impact for a wide range of both current as well as future technologies and standards. This would include cognitive radio standards such as IEEE 802.22, cellular technologies such as LTE and WiMAX, and perhaps even in femtocells and ad-hoc networking.

In future work, we plan to pursue a realtime implementation of blind IA by transferring the heavy computations to the FPGA module of the FlexRIO. Furthermore, we also aim to investigate the benefit of switching between multiple antennas (> 2) using an external RF switch.

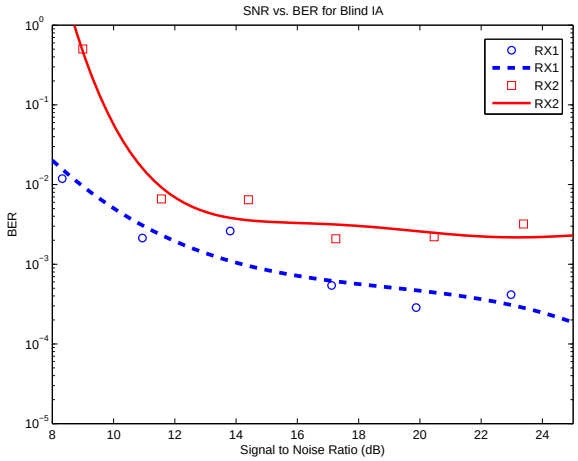

(a) SNR vs. BER at RX1 and RX2 for the blind IA scheme

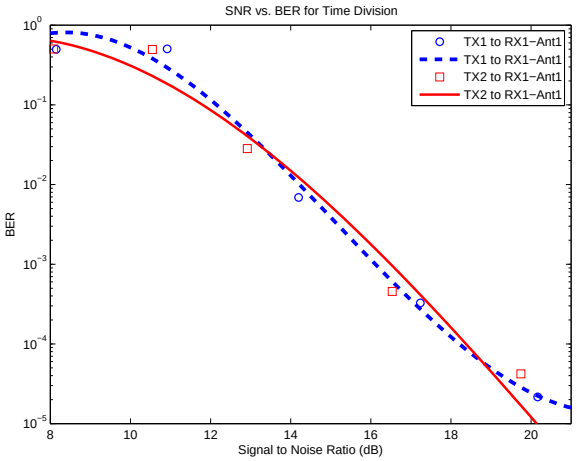

(b) SNR vs. BER at RX1 (using antenna 1) for the time-division scheme

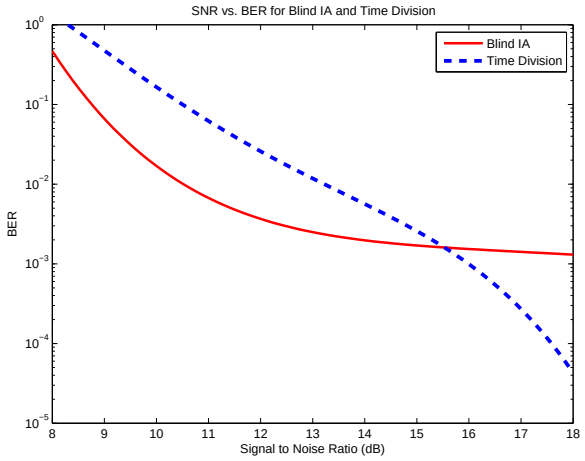

(c) SNR vs. BER for blind IA compared against time-division

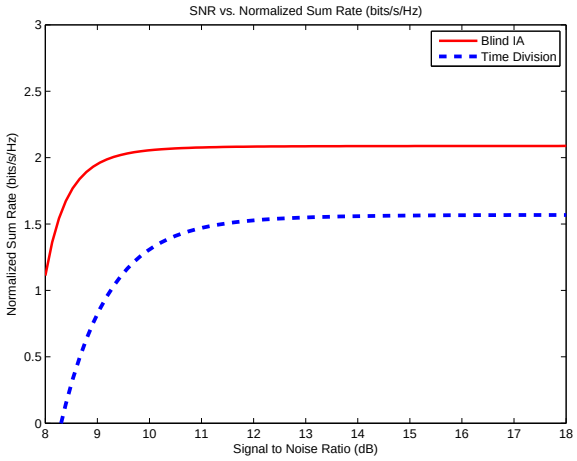

(d) SNR vs. R_{sum} for blind IA compared against time-division

Figure 6: Results from hardware implementation with $N = 600$ subcarriers

ACKNOWLEDGEMENT

The authors would like to thank Syed Jafar, Ian Wong, Christian Amadasun, Radha Ganti and Kumar Appaiah for very helpful discussions. The authors are also thankful to Harvey Cheng and Joshua Yuan for their help in code development.

[1] V.R. Cadambe and S.A. Jafar, "Interference Alignment and the Degrees of Freedom of the K-user Interference Channel," *IEEE Trans. Info. Theory*, Vol. 54, No. 8, pp. 3425–3441, Aug. 2008.

[2] M.A. Maddah-Ali, S.A. Motahari, and A.K. Khandani, "Communication over MIMO X Channels: Interference Alignment, Decomposition, and Performance Analysis," *IEEE Trans. on Information Theory*, Vol. 54, No. 8, pp. 3457-3470, Aug. 2008.

[3] S. Gollakota, S.D. Perli, and D. Katabi, "Interference alignment and cancellation," *SIGCOMM '09*, Aug. 2009.

[4] O. El Ayach, S.W. Peters, and R.W. Heath, Jr., ' 'The Feasibility of Interference Alignment Over Measured MIMO-OFDM Channels," submitted to *IEEE Trans. on Vehicular Technology*, *e-print arXiv:0911.1849v2*, Feb. 2010.

[5] C. Wang, T. Guo, and S.A. Jafar, "Aiming Perfectly in the Dark - Blind Interference Alignment through Staggered Antenna Switching," *e-print arXiv:1002.2720*, Feb. 2010.

[6] S. Jafar and S. Shamai, "Degrees of Freedom Region for the MIMO X Channel," *IEEE Trans. on Information Theory*, Vol. 54, No. 1, pp. 151–170, Jan. 2008.

[7] 3GPP, *3GPP TS 36.211 V8.9.0 E-UTRA Physical Channels and Modulation (Release 8)*, 2008.

[8] National Instruments, "NI PXIe-1082 User Manual", [Online] http://www.ni.com/pdf/manuals/372752b.pdf, Feb. 2010.

[9] T.M. Schmidl and D.C. Cox, "Robust frequency and timing synchronization for OFDM," *IEEE Trans. on Communications*, Vol. 45, No. 12, pp. 1613–1621, Dec. 1997.